Title

Changes in Imaging and Cognition in Juvenile Rats After Whole-Brain Irradiation

Journal

International Journal of Radiation Oncology • Biology • Physics, 96(2)

ISSN

0360-3016

Authors

Brown, Robert J

Jun, Brandon J

Cushman, Jesse D

et al.

Publication Date

2016-10-01

DOI

10.1016/j.ijrobp.2016.06.013

Peer reviewed

HHS Public Access

Author manuscript

Int J Radiat Oncol Biol Phys. Author manuscript; available in PMC 2017 August 19.

Published in final edited form as:

Int J Radiat Oncol Biol Phys. 2016 October 01; 96(2): 470–478. doi:10.1016/j.ijrobp.2016.06.013.

Changes in Imaging and Cognition in Juvenile Rats After Whole-Brain Irradiation

Robert J. Brown, MD[*,†,‡], **Brandon J. Jun, BS**[*,†,‡], **Jesse D. Cushman, PhD**[§], **Christine Nguyen**[*], **Adam H. Beighley, BS**[*], **Johnny Blanchard, BS**[*], **Kei Iwamoto, PhD**[*], **Dorthe Schaue, PhD**[*], **Neil G. Harris, PhD**[‖], **James D. Jentsch, PhD**[§], **Stefan Bluml, PhD**[†,‡], and **William H. McBride, PhD, DSc**[*]

[*]Division of Molecular and Cellular Oncology, Department of Radiation Oncology, David Geffen School of Medicine, University of California, Los Angeles

[§]Department of Psychology, University of California, Los Angeles

[†]Advanced Imaging Laboratory, Department of Radiology, Children's Hospital Los Angeles

[‖]UCLA Brain Injury Research Center, Department of Neurosurgery, David Geffen School of Medicine at UCLA Center for the Health Sciences, Los Angeles, California

[‡]Rudi Schulte Research Institute, Santa Barbara, California

Abstract

Purpose—In pediatric cancer survivors treated with whole-brain irradiation (WBI), long-term cognitive deficits and morbidity develop that are poorly understood and for which there is no treatment. We describe similar cognitive defects in juvenile WBI rats and correlate them with alterations in diffusion tensor imaging and magnetic resonance spectroscopy (MRS) during brain development.

Methods and Materials—Juvenile Fischer rats received clinically relevant fractionated doses of WBI or a high-dose exposure. Diffusion tensor imaging and MRS were performed at the time of WBI and during the subacute (3-month) and late (6-month) phases, before behavioral testing.

Results—Fractional anisotropy in the splenium of the corpus callosum increased steadily over the study period, reflecting brain development. WBI did not alter the subacute response, but thereafter there was no further increase in fractional anisotropy, especially in the high-dose group. Similarly, the ratios of various MRS metabolites to creatine increased over the study period, and in general, the most significant changes after WBI were during the late phase and with the higher dose. The most dramatic changes observed were in glutamine-creatine ratios that failed to increase normally between 3 and 6 months after either radiation dose. WBI did not affect the ambulatory response to novel open field testing in the subacute phase, but locomotor habituation was impaired

Reprint requests to: William H. McBride, PhD, DSc, Department of Radiation Oncology, David Geffen School of Medicine, University of California, Los Angeles, 10833 LeConte Ave, B3-109 CHS, Los Angeles, CA 90095. Tel: (310) 825-4584; wmcbride@mednet.ucla.edu.

Conflict of interest: none.

and anxiety-like behaviors increased. As for cognitive measures, the most dramatic impairments were in novel object recognition late after either dose of WBI.

Conclusions—The developing brains of juvenile rats given clinically relevant fractionated doses of WBI show few abnormalities in the subacute phase but marked late cognitive alterations that may be linked with perturbed MRS signals measured in the corpus callosum. This pathomimetic phenotype of clinically relevant cranial irradiation effects may be useful for modeling, mechanistic evaluations, and testing of mitigation approaches.

Introduction

Whole-brain irradiation (WBI) for children with cancer leads to profound lifelong morbidity and early death (1), including endocrinopathies (2), cerebrovascular disease (3), and advanced brain aging (4), leading to progressive declines in IQ (5–7), decreased academic achievement (8), reduced earning potential, and poorer quality of life (9), Because approximately one-quarter of all pediatric patients who have received cranial irradiation now survive, assessing radiation-induced damage to the developing brain is critical for treatment and planning strategies (10). Known risk factors include age at treatment (1, 11, 12) and radiation dose (6). Conformal radiation treatment planning (13, 14) and particle radiation therapy (15) may reduce the total hippocampal dose but are of limited value where extensive areas of the brain have to be treated (16).

Animal models demonstrate several potential mechanisms of injury after WBI, including cerebrovasculature injury (17, 18), loss of neuronal progenitors (19, 20), white matter injury (21, 22), and persistent inflammation (23). Responses evolve over time, with most serious symptoms being expressed during the subacute and late phases, which may have different pathologic mechanisms (23); the latter are considered irreversible. Little is known about how the developing brain responds to clinical fractionated WBI, with most data coming from animal models using adults and single dose fractions, which may mislead (24, 25). In this study we follow imaging and cognitive subacute and late responses in the developing brains of juvenile rats to a clinically relevant course of fractionated WBI similar to what is used to treat children with high-risk medulloblastoma.

Methods and Materials

All studies were approved by the Institutional Animal Care and Use Committee and performed in accordance with federal National Institutes of Health guidelines. An experimental schema is presented in Figure 1. Twenty-eight– day–old male Fischer rats (Harlan Laboratories, Indianapolis, IN) received sham WBI (0 Gy) or received either 27 Gy in 9 daily fractions of 3 Gy, which is bioeffective with 34 Gy in 1.8-Gy clinical fractions (linear-quadratic model, $\alpha/\beta = 3$ Gy) (26, 27), or 34 Gy, where the last 3-Gy fraction was replaced with a 10-Gy boost. Animals were anesthetized with ketamine and zylazine (intraperitoneally) and positioned laterally on a platform shielded with a Cerrobend (Radiation Products Design, Inc, Albertville, MN) jig exposing the cranium. Radiation was delivered using a Gulmay RS320 x-ray unit (Gulmay Medical, Surrey, UK) with the following parameters: 1.5-mm copper and 3-mm aluminum filters, 300 kV at 10 mA, dose rate of 1.173 Gy/min, and focus to skin distance of 42.3 cm. To avoid radiation injury to the

oral mucosa, radiation was delivered laterally across the brain. To account for any drop-off in radiation dose over the width of the entire brain, the daily dose was delivered using 2 beams, 1 entering the right hemisphere and 1 entering the left hemisphere. This was accomplished by first positioning the animal with the right hemisphere toward the source. After delivery of half of the daily dose, the animals were turned over with the left hemisphere toward the source for delivery of the second half of the daily radiation dose. Thus any difference in dose from the point of entry of one side of the brain to the opposite was balanced daily. This radiobiological technique was used to equalize the dose across the entire volume of the target organ. Weekly dosimetry used both film (Gafchromic EBT2; International Specialty Products, Wayne, NJ) and a Harshaw TLD-100H (lithium fluoride–magnesium, copper, phosphorus, (Thermo Fisher Scientific, Waltham, MA)). calibrated dosimeter.

Magnetic resonance imaging (MRI) used a 7-Tesla field (Bruker BioSpin, Billerica, MA; 116-mm inner diameter; maximum gradient strength of 400 mT/m) and interfaced with a 300-MHz resonant frequency digital spectrometer. Signal excitation and reception used a cross-coil system with a 7–cm–inner diameter linear birdcage and surface coils, respectively. Animals were anesthetized with isoflurane and stabilized with tooth holder and ear clamps with continuous monitoring of respiratory rate and body temperature. Diffusion tensor imaging (DTI)–echo planar imaging data were acquired with the following parameters: repetition time, 6250 ms; echo time, 23 ms; 1 echo; echo spacing, 0.5 ms; flip angle, 90°; bandwidth, 246,914 Hz; and slice thickness, 0.75 mm using a nominal b value of 700. Fractional anisotropy (FA) maps were constructed using FSL software (FMRIB Software Library v5.0, Oxford, UK). By use of the axial slice closest to bregma −4.0, a 16 × 8–pixel region of interest (ROI) was centered on the identifiable corpus callosum and pixels with an FA value >0.5 were defined for analysis (Fig. 2A). Proton magnetic resonance spectroscopy (MRS) data were obtained from a $3 \times 6 \times 2$–mm^3 voxel overlying the corpus callosum and a $3 \times 3 \times 3$–mm^3 voxel overlying the right hippocampus using 2 double spin echo point-resolved spectroscopy sequences, one with water suppression and one without (echo time, 20 ms; repetition time, 2500 ms; 324 averages). Second-order shimming was achieved using the fast, automatic shimming technique by mapping along projections (FASTMAP) technique. MRS data curve fitting and quantitation of metabolite levels were performed by use of LCModel software (S. Provencher, Oakville, Ontario, Canada), and spectra were rejected if the full width at half maximum was >0.1 ppm or the signal-to-noise ratio was <6 —objective measures of data quality automatically reported by the processing software—or if a data shift along the ppm axis was >2 SDs of the remaining scans (−0.87 < ppm shift < 0.053). Finally, outliers of the 7 predetermined metabolites defined as > or <2 SDs were excluded. The metabolite levels quantified were as follows: total creatine (creatine + phosphocreatine); glutamine; glutamate; total choline (choline + phosphocholine); total NAA (*N*-acetylaspartate + *N*-acetylaspartylglutamate); total lactate (lactate + lipids 13a + lipids 13b); and myoinositol. The rationale for normalizing metabolite levels to their respective time and ROI levels was to obtain the most robust markers. In contrast to absolute quantitation, the impact of changes in the water content and of metabolite relaxation times on metabolite ratios is small. To show potential differences over development, the 3- and 6-month ratios were further normalized to their baseline values.

The investigators were blinded with respect to treatment group for behavioral tests, MRS, and FA measurements and analysis. For lateralized reaction time tests, animals were maintained on caloric restriction (85% of 3-month baseline) beginning 2 months after WBI (28). Open field exploration (OFE) used a circular enclosure 120 cm in diameter with 48cm plain white plastic walls. Animals were allowed to freely explore the empty enclosure for 10 min/d for 2 days at 4 months after WBI and for 1 day at 7 months. Total distance and percent of time in the center were analyzed using TopScan analysis software (CleverSys, Reston, VA) and expressed in arbitrary units. Novel object recognition (NOR) was tested on 2 days after OFE in the same arena (29). Two identical objects were placed on opposite sides of the enclosure 10 cm from the wall. On day 1, animals underwent three 5-minute exploratory trials separated by 5-minute intervals. After 24 hours, one of the objects was replaced with a novel object, and the animal was allowed to explore for 5 minutes. The time of active exploration of each object was measured manually with stopwatches by an observer blinded to the treatment. A novel object preference ratio (Time exploring novel object − Time exploring familiar object)/(Time exploring novel object + Time exploring familiar object) was used for analysis. Testing with the elevated plus maze (EPM) was performed at 4 months after WBI and not repeated at 7 months because it relies on the novelty of the apparatus for maximal effect. Rats were placed in the center of a plus-shaped maze elevated 4 ft from the floor and allowed to freely explore for 5 minutes. Time spent in the open arms was measured with stopwatches.

The primary outcome measure for this study was the NOR task. Detecting an effect size of 0.25 among 3 groups using a repeated-measures (2 time points) analysis of variance (ANOVA) within-between interactions assuming a correlation of 0.5 and a nonsphericity correction of 1 indicated a total group size of 42. Adding 15% for attrition yielded a total of 48 animals, or 16 per group. Statistical analyses were carried out using SPSS statistical software (version 22; IBM, Armonk, NY) or Prism 6.0 (GraphPad Software, La Jolla, CA). ANOVA was first used to analyze all groups compared with pre-WBI values. If any F statistic was significant to $P<.05$, a post hoc Student t test was performed. Differences between baseline values were considered significant at $P<.05$, adjusted for multiple comparisons using the Dunnett test. All measurements are reported as means ± 1 SEM unless otherwise specified.

Results

Mean weight of animals at 28 days of age was similar for all groups. However, irradiated animals weighed less than sham animals by 6 months after WBI (0 Gy, 355 ± 7 g; 27 Gy, 325 ± 6 g; 34 Gy, 309 ± 6 g; $F_{2,43} = 12.66$, $P<.0001$).

MRI showed no gross abnormalities up to 6 months after WBI in all animals. At 6 months, the areas of corpus callosum defined as ROIs consisting of pixels with FA values >0.5 at bregma −4.0 were similar between 0 Gy (1.80 ± 0.05 mm^2) and 34 Gy (1.83 ± 0.03 mm^2) ($P= .64$). The mean FA value of the corpus callosum increased in the sham-irradiated group over time ($P= .001$ at 3 months and $P<.0001$ at 6 months; Fig. 2B) and this was not affected by WBI up to the subacute phase (3 months after WBI); however, thereafter, there was no

further increase so that mean FA in the 34-Gy group was significantly lower than that in sham controls at 6 months ($P = .01$), suggesting late white matter injury.

The metabolite-creatine ratios measured in both the corpus callosum and right hippocampus are presented in Table 1. In the hippocampus, only the choline and glutamate ratios increased with age, whereas in the corpus callosum, most metabolite ratios did so. Figure 3 shows representative magnetic resonance spectra obtained from the corpus callosum. Interestingly, WBI did not affect measures in the hippocampus, whereas there were many changes in the corpus callosum (Fig. 4). By 6 months, glutamine-creatine ratios had increased dramatically with age (baseline vs 0 Gy, $P = .0066$; Fig. 4A) but this increase was not observed in either irradiated group. In contrast, increases in glutamate, glutamine, and total NAA (*N*-acetylaspartate + *N*-acetylaspartylglutamate) were delayed at 3 months after high, but not more clinically relevant, doses of WBI. There were no significant time- or dose-related changes in either lactate or myoinositol ratios.

Given the increased prevalence of attention-deficit disorder in brain tumor survivors, we assessed performance of sustained, divided attention using lateralized reaction time tests. Unfortunately, the variance within the groups was unexpectedly high and this resulted in no significant differences (data not shown); the test was abandoned. The results of the other behavioral tests are presented in Table 2 and Figure 5. In OFE assessment during the subacute period at 4 months, all groups were similarly active on day 1. However, on day 2, when sham-irradiated controls showed the expected reduction in exploratory activity ($P = .02$), animals receiving either 27-Gy or 34-Gy WBI failed to habituate ($P = .778$ and $P = .294$, respectively; Fig. 5A). By 7 months, all groups showed a similar decrease in day 1 exploratory behavior ($P < .0001$; Fig. 5B), possibly reflecting the effect of repeated exposures to the arena in all groups. They also showed more anxiety-like behavior in the EPM test, spending less time in the open arms relative to controls ($P = .002$ for 27 Gy and $P = .02$ for 34 Gy; Fig. 5C).

NOR was initially performed with plastic object pairs; however, control animals failed to show a significant preference for the novel object ($F_{1,14} = 1.064$, $P = .320$), but glass object pairs were effective ($F_{1,14} = 23.350$, $P < .0001$). This subsequent exclusion of plastic object trials underpowered the control sample size, but because the sham-irradiated controls from the 4- and 7-month tests showed equivalent high-level NOR, indicating no effect of time on performance (preference ratios of 0.623 ± 0.054 at 4-month test and 0.559 ± 0.078 at 7 months; $P = .69$, *t* test), data were pooled for comparisons. At 4 months, both the 27-Gy and 34-Gy groups showed similar NOR preference to controls ($P = .826$ and $P = .807$, respectively; Fig. 5D), but by 7 months, NOR was impaired at both doses ($P = .021$ and $P = .021$, respectively). An overall ANOVA with the pooled sham controls and the 2 irradiated groups for the 4- and 7-month time points indicated an overall main effect ($F_{4,42} = 2.670$, $P = .047$). We explored the possibility that we failed to detect a difference at the 4-month time point because of a lack of power associated with the smaller sample size. The power required to detect a difference of similar magnitude to that observed at 7 months (observed effect sizes of 1.1 for 27 Gy and 1.2 for 34 Gy) was estimated by a post hoc power calculation with the lowest sample size (ie, 20). A 1-way ANOVA with N = 20 divided into 5 groups has a power of 0.88 to detect an effect of 1 with an α error of .05. Although these

data do not exclude some degree of NOR impairment at 4 months, one as large as that seen at 7 months is highly unlikely.

Discussion

We report imaging and cognitive effects of WBI in the developing brains of juvenile rats during the subacute and late periods after WBI using a clinically relevant dose and a higher dose of fractionated irradiation. FA levels in the corpus callosum of sham-irradiated rats increased over the study period, consistent with normal white matter development, and WBI did not affect this up to at least 3 months. However, the later increase was blunted after high-dose WBI (34 Gy). In children and adults who survive radiation therapy for brain cancer, decreases in FA in white matter have been reported (30, 31). In rats, other authors have variably shown a decrease in FA in the corpus callosum 1 year after large single WBI doses (32) or no change after fractionated irradiation with larger bioequivalent doses than we used (33, 34). Further work is needed using clinically relevant doses at later time points and including other diffusion tensor imaging parameters, such as mean diffusivity, and areas other than the corpus callosum, such as the fimbria, that have been implicated in hippocampal impairment (35) before the value of MRI in imaging white matter changes can be fully evaluated.

MRS, on the other hand, has been shown to demonstrate metabolic alterations associated with brain injury before structural changes have emerged (36). We investigated changes in the metabolic profiles in both the hippocampus and corpus callosum of juvenile rats after WBI. The hippocampus showed no changes that could be attributed to irradiation, which is consistent with the findings of Robbins et al (37) in adult rats. In contrast, the corpus callosum showed significant WBI-associated alterations in metabolic profiles. Developmental changes were observed with most metabolites that were either delayed or completely prevented by high-dose WBI. Most noteworthy was the blunting of the increase in the glutamine ratios late after both clinically relevant and high radiation doses–the time when NOR is impaired. Glutamine, the most abundant amino acid in the cerebrospinal fluid, is synthesized by astrocytes and is generally reported in combination with glutamate because of their interdependency in neuronal-glial interactions. In contrast, glutamate is primarily synthesized by neurons and metabolized to glutamine by astrocytes (38). Disruption of glutamine synthesis has been associated with viral-induced astrocytic gliosis that may lead to neuronal dysfunction and may serve as a marker of clinically significant injury (39).

Prefrontal lobe dysfunction after WBI is suggested by reports of an increased incidence of attention-deficit disorder and impairment in both executive function and working memory after childhood radiation therapy for cancer (40, 41). Because this can impair school learning, it has been postulated that addressing prefrontal dysfunction may improve overall outcome and radiation-induced loss in IQ (42, 43). Our study showed that both WBI doses caused decreased exploratory behavior in the EPM test and prevented habituation in OFE at 4 months by rats, which is suggestive of early-onset prefrontal dysfunction. NOR, on the other hand, is most often used to measure hippocampal-independent working memory; however, in our test, with a 24-hour interval, it is hippocampal dependent (44). Our demonstration that NOR is not affected 4 months after WBI but is dramatically impaired at

the late time point may be the first demonstration of hippocampal-dependent declarative non-spatial memory deficit following clinically relevant fractionated juvenile WBI. Several studies have shown impairment in this task using short intersession delays, but these more likely reflect prefrontal dysfunction than longterm memory impairment (37, 45–48). A limitation of our observation that NOR is normal at 4 months after WBI is the small number of animals, as described in the Results section. However, a post hoc power calculation indicated that any difference in the subacute phase is likely to be much less than that observed in the late phase. Throughout, our studies point to the conclusion that subacute deficits in the developing brain after WBI are markedly less than those during the late phase, which is perhaps surprising.

In summary, we report imaging and behavioral outcomes of clinically relevant fractionated WBI in the prepubescent male rat that are consistent with observations in survivors of pediatric cancer treated in a similar manner. We further show that prefrontal dysfunction may antecede long-term memory impairment but may not necessarily be related to long-term cognitive dysfunction. The finding that WBI interferes with the normal increase of glutamine concentration in the corpus callosum suggests that injury to this structure may contribute to defects in hippocampal-dependent declarative memory, as has been suggested in the cortical-hippocampal system (49). Finally, these observations may serve as a suitable preclinical platform to link clinically relevant outcomes and histologic pathogenesis, as well as to evaluate radiation mitigation strategies.

Acknowledgments

Funding was provided by University of California, Los Angeles Jonsson Comprehensive Cancer Center, National Institutes of Health (NIH)/National Center for Advancing Translational Science, and University of California, Los Angeles Clinical and Translational Science Institute grant No. UL1TR000124 (R.J.B. and W.H.M.); Southern California Clinical and Translational Science Institute (NIH/National Center for Research Resources/National Center for Advancing Translational Science) grant No. KL2TR000131 (R.J.B.); National Institute of Allergy and Infectious Diseases, Center for Medical Countermeasures against Radiation grant No. U19AI067769 (W.H.M.); and the Rudi Schulte Research Institute (R.J.B., B.J.J., and S.B.). The authors are grateful for generous support from the Brain Mapping Medical Research Organization, Brain Mapping Support Foundation, Pierson-Lovelace Foundation, The Ahmanson Foundation, Capital Group Companies Charitable Foundation, William M. and Linda R. Dietel Philanthropic Fund, and Northstar Fund. Research reported in this publication was also partially supported by the National Center for Research Resources and by the Office of the Director of the NIH under award Nos. C06RR012169, C06RR015431, and S10OD011939.

References

1. Bloom HJ, Wallace EN, Henk JM. The treatment prognosis of medulloblastoma in children A study of 82 verified cases. Am J Roentgenol Radium Ther Nucl Med. 1969; 105:43–62.
2. Merchant TE, Conklin HM, Wu S, et al. Late effects of conformal radiation therapy for pediatric patients with low-grade glioma: Prospective evaluation of cognitive, endocrine, and hearing deficits. J Clin Oncol. 2009; 27:3691–3697. [PubMed: 19581535]
3. Bowers DC, Liu Y, Leisenring W, et al. Late-occurring stroke among long-term survivors of childhood leukemia and brain tumors: A report from the Childhood Cancer Survivor Study. J Clin Oncol. 2006; 24:5277–5282. [PubMed: 17088567]
4. Edelstein K, Spiegler BJ, Fung S, et al. Early aging in adult survivors of childhood medulloblastoma: Long-term neurocognitive, functional, and physical outcomes. Neuro Oncol. 2011; 13:536–545. [PubMed: 21367970]
5. Hirsch JF, Renier D, Czernichow P, et al. Medulloblastoma in childhood. Survival and functional results. Acta Neurochir (Wien). 1979; 48:1–15. [PubMed: 495234]

6. Mulhern RK, Palmer SL, Merchant TE, et al. Neurocognitive consequences of risk-adapted therapy for childhood medulloblastoma. J Clin Oncol. 2005; 23:5511–5519. [PubMed: 16110011]
7. Ris MD, Walsh K, Wallace D, et al. Intellectual and academic outcome following two chemotherapy regimens and radiotherapy for average-risk medulloblastoma: COG A9961. Pediatr Blood Cancer. 2013; 60:1350–1357. [PubMed: 23444345]
8. Palmer SL, Reddick WE, Gajjar A. Understanding the cognitive impact on children who are treated for medulloblastoma. J Pediatr Psychol. 2007; 32:1040–1049. [PubMed: 17329318]
9. Palmer SL. Neurodevelopmental impact on children treated for me-dulloblastoma: A review and proposed conceptual model. Dev Disabil Res Rev. 2008; 14:203–210. [PubMed: 18924159]
10. Oeffinger KC, Mertens AC, Sklar CA, et al. Chronic health conditions in adult survivors of childhood cancer. N Engl J Med. 2006; 355:1572–1582. [PubMed: 17035650]
11. Chin HW, Maruyama Y. Age at treatment and long-term performance results in medulloblastoma. Cancer. 1984; 53:1952–1958. [PubMed: 6704921]
12. Hoppe-Hirsch E, Renier D, Lellouch-Tubiana A, et al. Medulloblastoma in childhood: Progressive intellectual deterioration. Childs Nerv Syst. 1990; 6:60–65. [PubMed: 2340529]
13. Blomstrand M, Brodin NP, Munck Af, Rosenschöld P, et al. Estimated clinical benefit of protecting neurogenesis in the developing brain during radiation therapy for pediatric medulloblastoma. Neuro Oncol. 2012; 14:882–889. [PubMed: 22611031]
14. Brodin NP, Munck Af, Rosenschöld P, Blomstrand M, et al. Hippocampal sparing radiotherapy for pediatric medulloblastoma: Impact of treatment margins and treatment technique. Neuro Oncol. 2014; 16:594–602. [PubMed: 24327585]
15. Kuhlthau KA, Pulsifer MB, Yeap BY, et al. Prospective study of health-related quality of life for children with brain tumors treated with proton radiotherapy. J Clin Oncol. 2012; 30:2079–2086. [PubMed: 22565004]
16. Gudrunardottir T, Lannering B, Remke M, et al. Treatment developments and the unfolding of the quality of life discussion in childhood medulloblastoma: A review. Childs Nerv Syst. 2014; 30:979–990. [PubMed: 24569911]
17. Reinhold HS, Calvo W, Hopewell JW, et al. Development of blood vessel-related radiation damage in the fimbria of the central nervous system. Int J Radiat Oncol Biol Phys. 1990; 18:37–42. [PubMed: 2298633]
18. Brown WR, Thore CR, Moody DM, et al. Vascular damage after fractionated whole-brain irradiation in rats. Radiat Res. 2005; 164:662–668. [PubMed: 16238444]
19. Hopewell JW, Cavanagh JB. Effects of X irradiation on the mitotic activity of the subependymal plate of rats. Br J Radiol. 1972; 45:461–465. [PubMed: 5029031]
20. Monje ML, Mizumatsu S, Fike JR, et al. Irradiation induces neural precursor-cell dysfunction. Nat Med. 2002; 8:955–962. [PubMed: 12161748]
21. Chiang CS, McBride WH, Withers HR. Myelin-associated changes in mouse brain following irradiation. Radiother Oncol. 1993; 27:229–236. [PubMed: 7692473]
22. Panagiotakos G, Alshamy G, Chan B, et al. Long-term impact of radiation on the stem cell and oligodendrocyte precursors in the brain. PLoS One. 2007; 2:e588. [PubMed: 17622341]
23. McBride WH. Cytokine cascades in late normal tissue radiation responses. Int J Radiat Oncol Biol Phys. 1995; 33:233–234. [PubMed: 7642425]
24. Blomstrand M, Kalm M, Grandér R, et al. Different reactions to irradiation in the juvenile and adult hippocampus. Int J Radiat Biol. 2014; 90:807–815. [PubMed: 25004947]
25. Greene-Schloesser DM, Kooshki M, Payne V, et al. Cellular response of the rat brain to single doses of (137)Cs γ rays does not predict its response to prolonged “biologically equivalent” fractionated doses. Int J Radiat Biol. 2014; 90:790–798. [PubMed: 24937374]
26. Fowler JF. The linear-quadratic formula and progress in fractionated radiotherapy. Br J Radiol. 1989; 62:679–694. [PubMed: 2670032]
27. Lawrence YR, Li XA, el Naqa I, et al. Radiation dose-volume effects in the brain. Int J Radiat Oncol Biol Phys. 2010; 76(Suppl):S20–S27. [PubMed: 20171513]

28. Jentsch JD, Aarde SM, Seu E. Effects of atomoxetine and methylphenidate on performance of a lateralized reaction time task in rats. Psychopharmacology (Berl). 2009; 202:497–504. [PubMed: 18535818]
29. Ennaceur A, Delacour J. A new one-trial test for neurobiological studies of memory in rats. 1: Behavioral data. Behav Brain Res. 1988; 31:47–59. [PubMed: 3228475]
30. Mabbott DJ, Noseworthy MD, Bouffet E, et al. Diffusion tensor imaging of white matter after cranial radiation in children for medulloblastoma: Correlation with IQ. Neuro Oncol. 2006; 8:244–252. [PubMed: 16723629]
31. Palmer SL, Glass JO, Li Y, et al. White matter integrity is associated with cognitive processing in patients treated for a posterior fossa brain tumor. Neuro Oncol. 2012; 14:1185–1193. [PubMed: 22898373]
32. Wang S, Wu EX, Qiu D, et al. Longitudinal diffusion tensor magnetic resonance imaging study of radiation-induced white matter damage in a rat model. Cancer Res. 2009; 69:1190–1198. [PubMed: 19155304]
33. Peiffer AM, Shi L, Olson J, et al. Differential effects of radiation and age on diffusion tensor imaging in rats. Brain Res. 2010; 1351:23–31. [PubMed: 20599817]
34. Peiffer AM, Creer RM, Linville C, et al. Radiation-induced cognitive impairment and altered diffusion tensor imaging in a juvenile rat model of cranial radiotherapy. Int J Radiat Biol. 2014; 90:799–806. [PubMed: 24991879]
35. Aggleton JP, Brown MW. Episodic memory, amnesia, and the hippocampal-anterior thalamic axis. Behav Brain Sci. 1999; 22:425–444. discussion 444–489. [PubMed: 11301518]
36. Robbins ME, Brunso-Bechtold JK, Peiffer AM, et al. Imaging radiation-induced normal tissue injury. Radiat Res. 2012; 177:449–466. [PubMed: 22348250]
37. Robbins ME, Payne V, Tommasi E, et al. The AT1 receptor antagonist, L-158,809, prevents or ameliorates fractionated whole-brain irradiation-induced cognitive impairment. Int J Radiat Oncol Biol Phys. 2009; 73:499–505. [PubMed: 19084353]
38. Bak LK, Schousboe A, Waagepetersen HS. The glutamate/GABA-glutamine cycle: Aspects of transport, neurotransmitter homeostasis and ammonia transfer. J Neurochem. 2006; 98:641–653. [PubMed: 16787421]
39. Ortinski PI, Dong J, Mungenast A, et al. Selective induction of astrocytic gliosis generates deficits in neuronal inhibition. Nat Neurosci. 2010; 13:584–591. [PubMed: 20418874]
40. Spiegler BJ, Bouffet E, Greenberg ML, et al. Change in neuro-cognitive functioning after treatment with cranial radiation in childhood. J Clin Oncol. 2004; 22:706–713. [PubMed: 14966095]
41. Mabbott DJ, Penkman L, Witol A, et al. Core neurocognitive functions in children treated for posterior fossa tumors. Neuropsychology. 2008; 22:159–168. [PubMed: 18331158]
42. Thompson SJ, Leigh L, Christensen R, et al. Immediate neurocognitive effects of methylphenidate on learning-impaired survivors of childhood cancer. J Clin Oncol. 2001; 19:1802–1808. [PubMed: 11251012]
43. Castellino SM, Tooze JA, Flowers L, et al. Toxicity and efficacy of the acetylcholinesterase (AChe) inhibitor donepezil in childhood brain tumor survivors: A pilot study. PediatrBlood Cancer. 2012; 59:540–547.
44. Cohen SJ, Munchow AH, Rios LM, et al. The rodent hippocampus is essential for nonspatial object memory. CurrBiol. 2013; 23:1685–1690.
45. Acharya MM, Christie L-A, Lan ML, et al. Rescue of radiation-induced cognitive impairment through cranial transplantation of human embryonic stem cells. Proc Natl Acad Sci USA. 2009; 106:19150–19155. [PubMed: 19901336]
46. Lee TC, Greene-Schloesser D, Payne V, et al. Chronic administration of the angiotensin-converting enzyme inhibitor, ramipril, prevents fractionated whole-brain irradiation-induced perirhinal cortex-dependent cognitive impairment. Radiat Res. 2012; 178:46–56. [PubMed: 22687052]
47. Forbes ME, Paitsel M, Bourland JD, et al. Early-delayed, radiation-induced cognitive deficits in adult rats are heterogeneous and age-dependent. Radiat Res. 2014; 182:60–71. [PubMed: 24937782]

48. Piao J, Major T, Auyeung G, et al. Human embryonic stem cell-derived oligodendrocyte progenitors remyelinate the brain and rescue behavioral deficits following radiation. Cell Stem Cell. 2015; 16:198–210. [PubMed: 25658373]

49. Eichenbaum H. A cortical-hippocampal system for declarative memory. Nat Rev Neurosci. 2000; 1:41–50. [PubMed: 11252767]

Summary

Few animal models of whole-brain irradiation take into account young age and dose fractionation. We present both imaging and behavioral data after clinically relevant fractionated whole-brain irradiation in juvenile rats pathomimetic to those observed in survivors of pediatric brain tumors including development of early prefrontal dysfunction and late memory deficits that correlate with developmental imaging abnormalities.

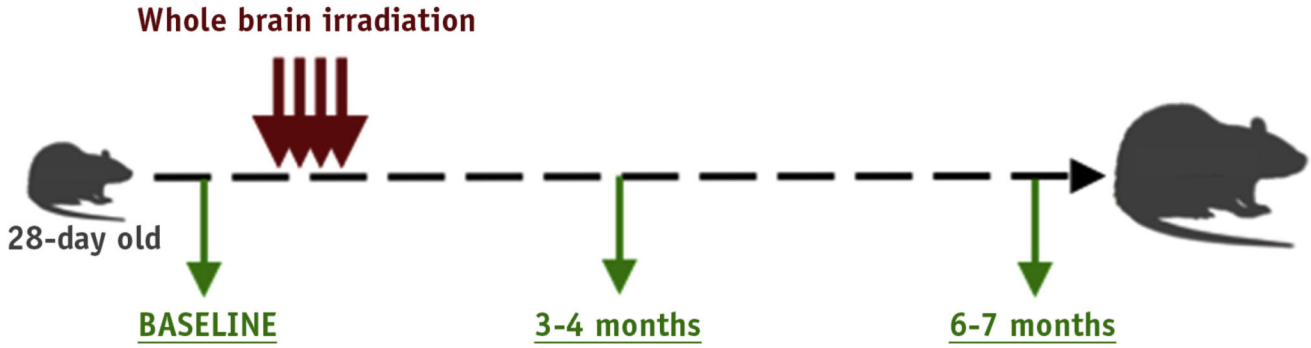

Fig. 1.

Experimental schema. Twenty-eight–day–old male. Fischer rats were irradiated over a period of 12 days. Baseline studies before irradiation included magnetic resonance imaging and spectroscopy. Imaging was repeated at 3 and 6 mo after irradiation. Behavioral testing was performed at 4 and 7 mo after irradiation.

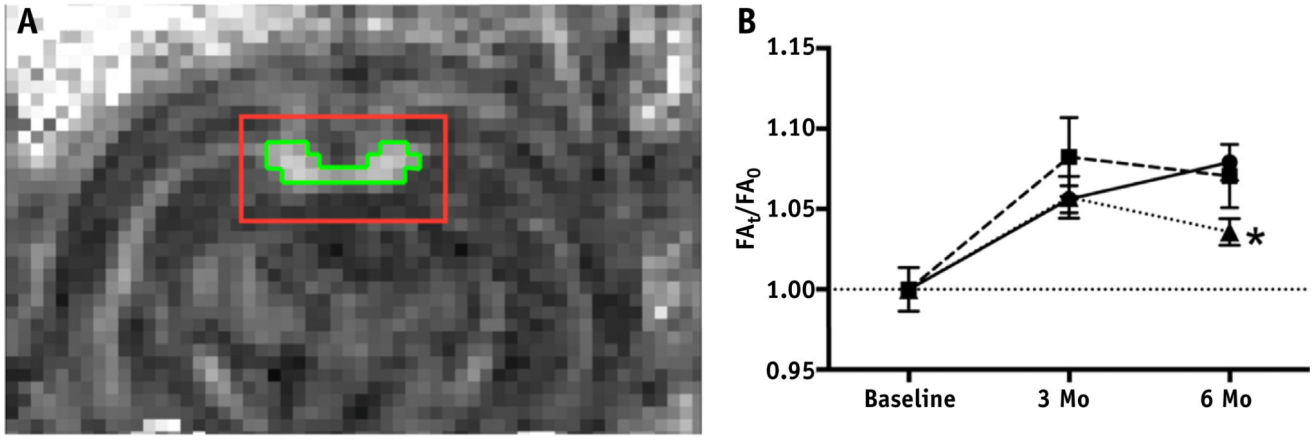

Fig. 2.

Fractional anisotropy (FA) of corpus callosum. (A) FA map of a representative coronal slice of a rat brain diffusion tensor image with corresponding region of interest (red outline) in which voxels with FA >0.5 (green outline) defined the measureable corpus callosum. (B) Plot of mean corpus callosum FA values relative to baseline (defined as FA_t/FA_0) for 0 Gy (circles), 27 Gy (squares), and 34 Gy (triangles). FA significantly increased from baseline for all groups (effect of group: $F_{6,89} = 5.300$, P=.0001). All animals had an increase in FA between baseline and 3 mo, indicating continued myelination, shown by plots >1 (relative to baseline: 0 Gy, P = .001; 27 Gy, P = .0001; and 34 Gy, P = .001). The 6-mo FA remained equivalent to 3-mo values for rats receiving 0 Gy of whole-brain irradiation (WBI), as well as rats receiving 27 Gy of WBI, but declined after 34-Gy WBI (0 Gy vs 34 Gy at 6 mo: P= .01). *P<.05. (A color version of this figure is available at www.redjournal.org.)

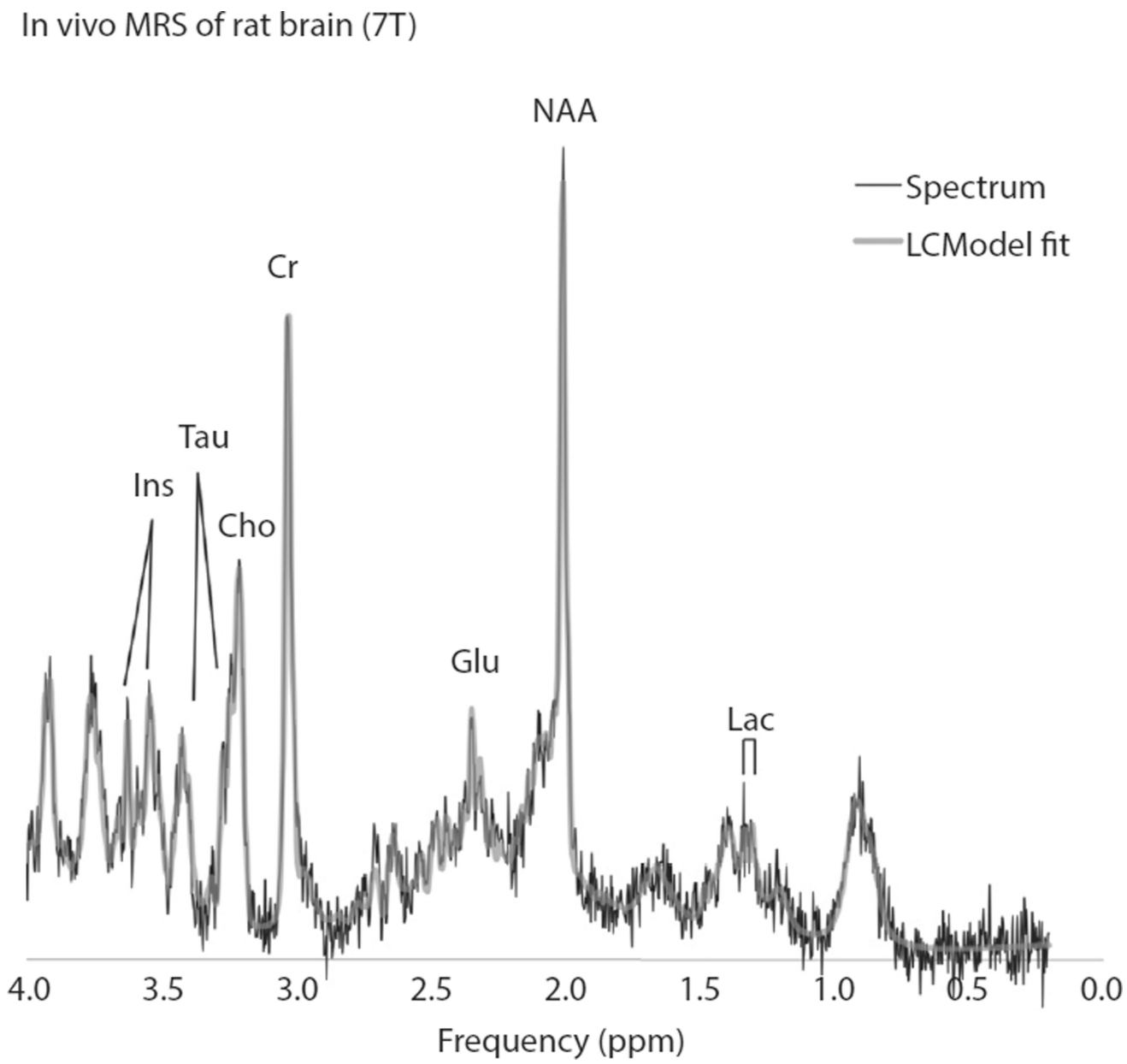

Fig. 3.

Representative proton magnetic resonance spectra (MRS) of corpus callosum.

Abbreviations: Cho = choline; Cr = creatine; Glu = glutamate; Lac = lactate; Ins = myoinositol; Tau = taurine; NAA = N-acetylaspartate.

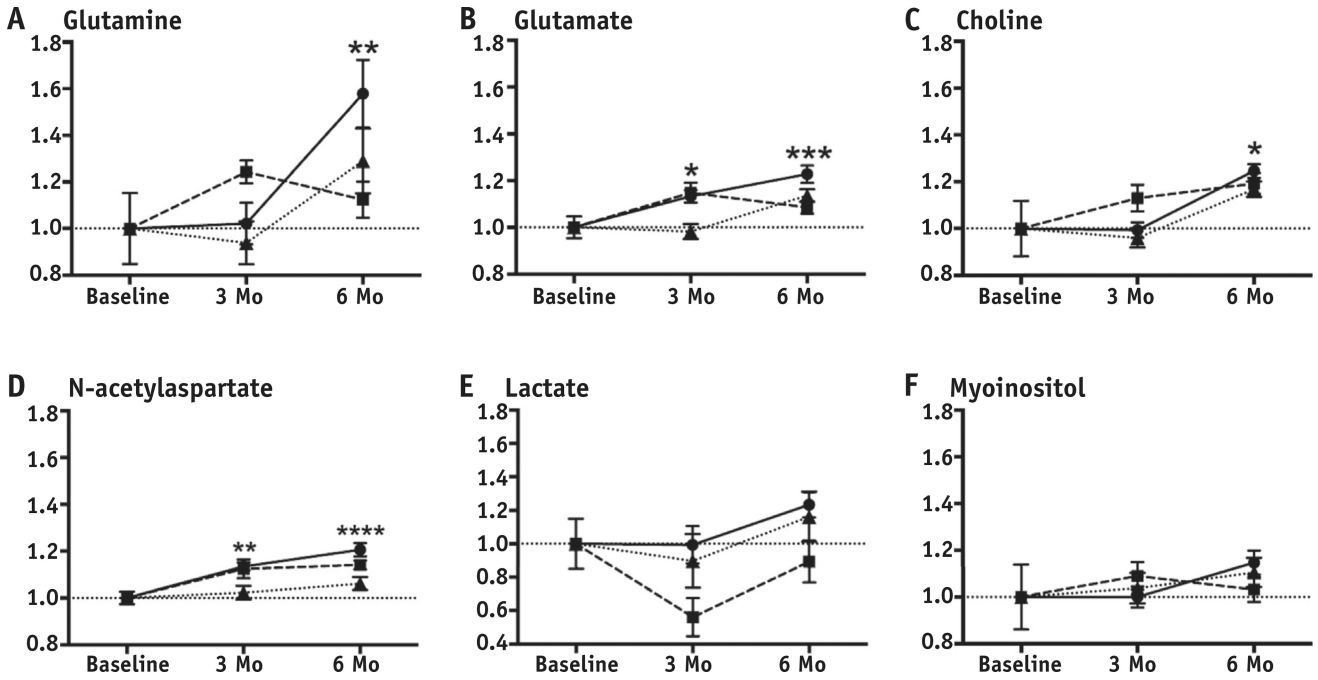

Fig. 4.

(A–F) Proton magnetic resonance spectroscopy metabolite-creatine ratios from corpus callosum plotted relative to baseline values for animals receiving 0 Gy (circles), 27 Gy (squares), and 34 Gy (triangles). **P*<.05, ***P*<.01, ****P*<.001, ****P<.0001.

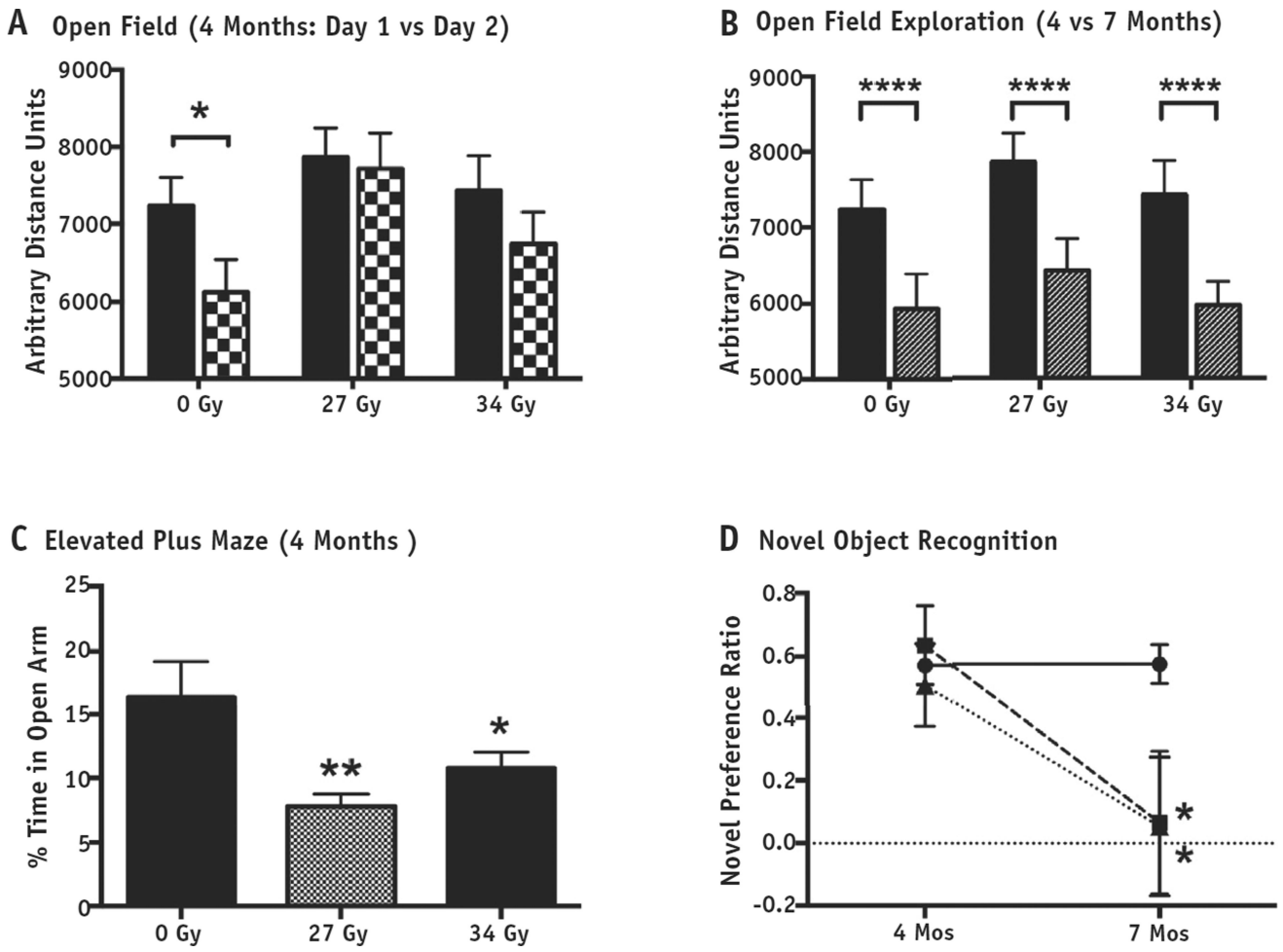

Fig. 5.

Behavioral testing. (A) The total distances moved in open field exploration by sham and whole-brain irradiation (WBI) rats on day 1 (solid bars) were equivalent (effect of group: $F_{2,46} = 0.591$, $P = .558$). A repeated-measures analysis of variance within each group was used to assess exploratory habituation on the second open field exposure (checkered bars). The control animals (0 Gy) showed a significant reduction in exploratory activity on day 2 relative to day 1 ($F_{1,13} = 7.036$, $P = .02$) unlike both WBI groups (27 Gy: $F_{1,15} = 0.083$, $P = .778$; 34 Gy: $F_{1,16} = 0.083$, $P = .294$). (B) Day 1 exploratory behavior was similar among groups at 4 mo (solid bars) and 7 mo (striped bars) but significantly decreased, indicating some retained familiarity with the arena (two-way analysis of variance on effect of time: $F_{1,81} = 17.09$, $P < .0001$). (C) The elevated plus maze showed significant decreases in time spent in the open arms by both WBI groups (overall effect of group: $F_{2,45} = 5.557$, $P = .007$; Least significant difference (LSD) planned post hoc comparisons relative to sham: $P = .002$ for 27 Gy and $P = .04$ for 34 Gy). (D) On the 24-h novel object recognition task, animals receiving 27 Gy (squares) and animals receiving 34 Gy (triangles) showed an overall main effect ($F_{4,42} = 2.670$, $P = .047$) when compared with pooled sham-irradiated controls (circles). Both the 27-Gy and 34-Gy groups showed normal novel object preference at 4 mo ($P = .826$

and $P = .807$, respectively) but impairment at 7 mo ($P = .02$ and $P = .02$, respectively). *$P < .05$, **$P < .01$, ***$P < .001$, ****$P < .0001$

Table 1

Mean (SEM) metabolite-creatine ratios

		3 mo after XRT (4 mo of age)			6 mo after XRT (7 mo of age)		
	P28: Baseline	**Control**	**27 Gy**	**34 Gy**	**Control**	**27 Gy**	**34 Gy**
Corpus callosum							
Gln[*,†]	0.38 (0.06)	0.39 (0.03)	0.48 (0.02)	0.36 (0.04)	0.61 (0.06)[†]	0.43 (0.03)	0.50 (0.05)
Glu[‡,§]	1.06 (0.05)	1.20 (0.03)[//]	1.21 (0.05)[//]	1.04 (0.03)	1.30 (0.04)[§]	1.15 (0.03)	1.20 (0.03)[//]
tCho[//,¶]	0.15 (0.02)	0.15 (0.01)	0.17 (0.01)	0.14 (0.01)	0.19 (0.01)[//]	0.18 (0.01)	0.17 (0.01)
NAA[§,#]	1.08 (0.03)	1.23 (0.02)[†]	1.22 (0.04)[//]	1.11 (0.03)	1.31 (0.03)[§]	1.24 (0.02)[//]	1.15 (0.03)
tLac[**]	0.48 (0.07)	0.48 (0.05)	0.27 (0.06)	0.43 (0.08)	0.59 (0.04)	0.43 (0.06)	0.56 (0.07)
mI[††]	0.55 (0.03)	0.55 (0.03)	0.59 (0.03)	0.57 (0.04)	0.63 (0.03)	0.56 (0.03)	0.60 (0.03)
Right hippocampus							
Gln[‡‡,§§]	0.39 (0.05)	0.56 (0.04)[//]	0.62 (0.03)[//]	0.46 (0.03)[//]	0.66 (0.04)[§]	0.57 (0.08)	0.59 (0.04)[†]
Glu[§,///]	1.12 (0.04)	1.36 (0.04)[§§]	1.36 (0.04)[†]	1.27 (0.04)[//]	1.39 (0.04)[§]	1.40 (0.06)[§§]	1.34 (0.03)[§§]
tCho[§,¶¶]	0.14 (0.01)	0.16 (0.01)	0.15 (0.01)	0.15 (0.01)	0.18 (0.01)[§§]	0.20 (0.01)[§]	0.17 (0.01)[†]
NAA[##]	1.11 (0.03)	1.21 (0.02)	1.18 (0.02)	1.16 (0.02)	1.17 (0.03)	1.20 (0.03)	1.13 (0.02)
tLac[***]	0.36 (0.04)	0.37 (0.05)	0.41 (0.15)	0.43 (0.04)	0.54 (0.06)	0.49 (0.12)	0.53 (0.06)
mI[†††]	0.55 (0.06)	0.58 (0.04)	0.55 (0.04)	0.53 (0.03)	0.63 (0.03)	0.63 (0.05)	0.55 (0.03)

Abbreviations: Gln = glutamine; Glu = glutamate; mI = myoinositol; NAA = *N*-acetylaspartate + *N*-acetylaspartylglutamate; tCho = total choline; tLac = total lactate; XRT = radiation therapy.

[*] $F_{6,64} = 3.131$, $P = .009$; post hoc *t* tests against baseline: 0 Gy at 6 mo, $P = .007$.

[†] $P < .01$.

[‡] $F_{6,64} = 5.996$, $P < .0001$; post hoc *t* tests against baseline: 0 Gy at 3 mo, $P = .036$; 27 Gy at 3 mo, $P = .42$; 0 Gy at 6 mo, $P < .0001$; 34 Gy at 6 mo, $P = .021$.

[§] $P < .0001$.

[//] $P < .05$.

[¶] $F_{6,64} = 2.878$, $P = .015$; post hoc *t* tests against baseline: 0 Gy at 6 mo, $P = .039$.

[#] $F_{6,64} = 7.199$, $P < .0001$; post hoc *t* tests against baseline: 0 Gy at 3 mo, $P = .003$; 27 Gy at 3 mo, $P = .022$; 0 Gy at 6 mo, $P < .0001$; 27 Gy at 6 mo, $P = .012$.

** $F_{6,64} = 2.028$, $P = .075$.

†† $F_{6,64} = 0.4592$, $P = .836$.

‡‡ $F_{6,69} = 5.105$, $P = .0002$; post hoc t tests against baseline: 0 Gy at 3 mo, $P = .014$; 27 Gy at 3 mo, $P = .014$; 0 Gy at 6 mo, $P < .0001$; 27 Gy at 6 mo, $P = .061$; Gy at 6 mo, $P = .004$.

§§ $P < .001$.

‖‖ $F_{6,69} = 6.762$, $P < .0001$; post hoc t tests against baseline: 0 Gy at 3 mo, $P = .0002$; 27 Gy at 3 mo, $P = .003$; 34 Gy at 3 mo, $P = .024$; 0 Gy at 6 mo, $P < .0001$; 27 Gy at 6 mo, $P = .0003$; 34 Gy at 6 mo, $P = .0003$.

¶¶ $F_{6,69} = 8.002$, $P < .0001$; post hoc t tests against baseline: 0 Gy at 6 mo, $P = .0003$; 27 Gy at 6 mo, $P < .0001$; 34 Gy at 6 mo, $P = .01$.

$F_{6,69} = 0.1.780$, $P = .116$.

*** $F_{6,69} = 1.487$, $P = .196$.

††† $F_{6,69} = 0.8460$, $P = .539$.

Table 2

Results of behavioral tests

	0 Gy	27 Gy	34 Gy
Open field			
4 mo, day 1			
Distance units ± SEM (n) [*]	7234 ± 368 (15)	7865 ± 379 (16)	7431 ± 453 (17)
% of time in center ± SEM (n) [†]	8.223 ± 1.336 (15)	9.094 ± 1.756 (16)	8.067 ± 1.168 (17)
4 mo, day 2,[‡]	6125 ± 427 (15)[§]	7714 ± 469 (16)	6740 ± 414 (17)
distance units ± SEM (n)			
7 mo, day 1,[‖,¶]	5934 ± 462 (12)	6423 ± 424 (15)	5966 ± 314 (13)
distance units ± SEM (n)			
Elevated plus maze (4 mo),[#,**]	16.4 ± 2.8 (15)	7.8 ± 1.0 (15) [**]	10.75 ± 1.3 (16)[§]
% of time in open arm ± SEM (n)			
Novel object recognition, preference ratio ± SEM (n)			
4 mo	0.572 ± 0.062 (14) [††]	0.636 ± 0.124 (4)	0.508 ± 0.134 (5)
7 mo[§,‡‡]	0.572 ± 0.062 (14) [††]	0.066 ± 0.228 (10)[§]	0.053 ± 0.221 (9)[§]

[*] Analysis of variance (ANOVA): $F_{2,45} = 0.6\ 1\ 9$, $P = .54$.

[†] ANOVA: $F_{2,45} = 0.150$, $P = .86$.

[‡] Repeated-measures ANOVA within each group between day 1 and day 2: 0 Gy, $F_{1,13} = 7.036$, $P = .02$; 27 Gy, $F_{1,15} = 0.083$, $P = .78$; 34 Gy, $F_{1,16} = 0.083$, $P = .29$.

[§] $P < .05$.

[‖] Two-way ANOVA of day 1 exploration distances at both 4 mo and 7 mo between groups—effect of time: $F_{1,81} = 17.09$, $P < .0001$; effect of dose: $F_{2,81} = 1.037$, $P = .36$; interaction: $F_{2,81} = 0.0221$, $P = .98$.

[¶] $P < .0001$.

[#] ANOVA—effect of group: $F_{2,45} = 5.557$, $P < .007$ (LSD post hoc t tests relative to 0 Gy: $P = .002$ for 27 Gy and $P = .04$ for 34 Gy).

[**] $P < .01$.

[††] Zero-gray novel object recognition tests were combined for analysis to increase power to evaluate for overall effect: 0-Gy preference ratios ± SEM at 4 mo (0.623 ± 0.054, n = 3) and 7 mo (0.559 ± 0.078, n = 11); t test of means between time points, $P = .69$.

[‡‡] ANOVA comparing 27 Gy and 34 Gy at each time point with pooled 0-Gy values—effect of group: $F_{4,37} = 2.679$, $P = .05$ (LSD post hoc t tests relative to pooled 0 Gy: $P = .02$ for 27 Gy at 6 mo and $P = .02$ for 34 Gy at 6 mo).